The role played by density in meso and large scale ocean dynamics

Mariana Miracca Lage

Advisor: Paulo S. Polito
Instituto Oceanográfico - Universidade de São Paulo

25 September 2020

Introduction

The ocean viewed from space

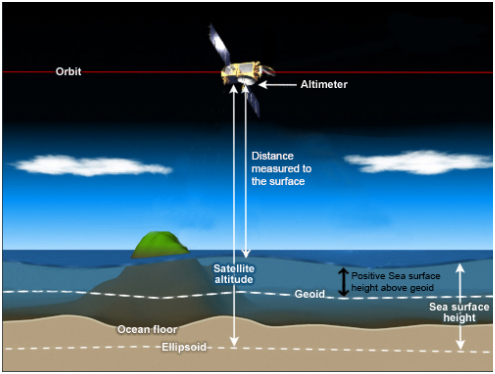

Simplified illustration of Satellite altimetry components. *European Space Agency*

- Large scale phenomena $\longleftarrow$ Electromagnetic radiation;
- Restricted to the ocean surface;
- Altimeters.

- 3D density field $\longrightarrow$ thermal wind;
- In a simple two-layer model, η variations are directly related to the interface displacements multiplied by $\frac{\Delta\rho}{\rho}$;
- Challenges $\longrightarrow$ Ocean General Circulation Models (GCM)

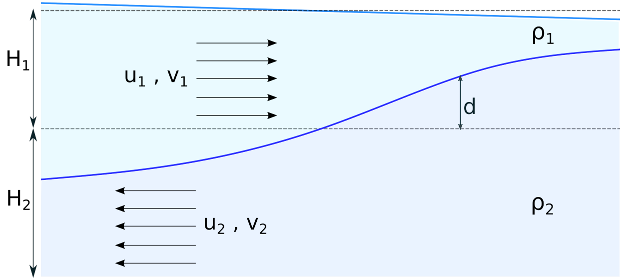

Altimeters × GCM

Aviso/Cmems

- Variable: Sea Surface Height (SSH)
- Resolution: 0.25° (∼30 km), 1 day
- Smoothed, interpolated data and noise

Hycom-Ncoda

- Variable: Sea Surface Height (SSH), experiment 53.X
- Resolution: 0.08° (∼10 km), 3 hours
- Less noise!

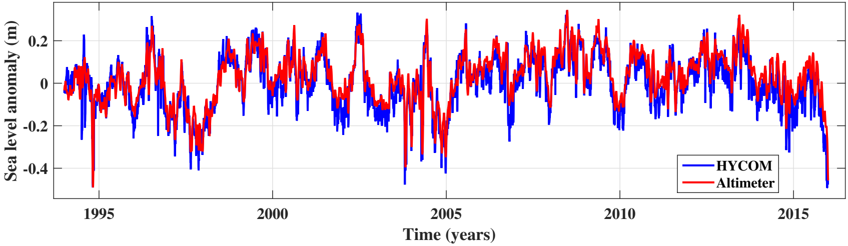

Time-series of sea surface height anomaly (SSHA) from the altimeter (red) and HYCOM (blue). Cross-correlation (0.8) performed from 1994 to 2015 at 15°N on the Pacific Ocean (test case).

Quasi-geostrophy and the Potential Vorticity Equation

Conservation of Potential Vorticity (PV)

$$\frac{\partial}{\partial t}\left[\nabla^2\psi + \beta y + \frac{\partial}{\partial z}\left(\frac{f_0^2}{N^2}\frac{\partial\psi}{\partial z}\right)\right] = 0\,.$$

From hydrostatics, at $z = 0$,

$$\frac{\partial\psi}{\partial z} = \frac{b_s}{f_0}.$$

Separation of variables $\longrightarrow$ Quasi-Geostrophy (QG) and Surface Quasi-Geostrophy (SQG).

Quasi-Geostrophy

- $b_s = 0$;
- Sturm-Liouville problem; λ_i is the separation constant, defined as R_{di}^{-2};

$$\frac{\partial}{\partial z}\left(\frac{f_0^2}{N^2}\frac{\partial F_i}{\partial z}\right) + \lambda_i F_i = 0$$

Boundary conditions:

$$\begin{cases} \frac{\partial F_i}{\partial z} = 0 \text{ @ } z = 0\,, \\ \frac{\partial F_i}{\partial z} = 0 \text{ @ } z = -H. \end{cases}$$

Surface Quasi-Geostrophy

- $b_s \neq 0$;
- Vertical transfer function (χ) dependent on the wavenumber K;

$$\frac{\partial}{\partial z}\left(\frac{f_0^2}{N^2}\frac{\partial \chi}{\partial z}\right) - K^2\chi = 0$$

Boundary conditions:

$$\begin{cases} \frac{\partial \chi}{\partial z} = 1 \text{ @ } z = 0\,, \\ \frac{\partial \chi}{\partial z} = 0 \text{ @ } z = -H. \end{cases}$$

Mesoscale

- L $\sim$ 10—100 km
- T $\sim$ weeks—months
- $R_o = O(10^{-2})$

SQG dynamics $\longrightarrow$ *Chapter 2*

Large scale

- L $\sim$ 100—1000 km
- T $\sim$ months—years
- $R_o = O(10^{-4})$

QG dynamics $\longrightarrow$ *Chapter 3*

Hypotheses and Objectives

Hypotheses

- **Chapter 2**:
  - H_1: The dominance of QG or SQG over Atlantic's SSH is related to the amount of mesoscale activity in each area;
- **Chapter 3**:
  - H_2: Most of the variability of the SSHA is explained by Rossby waves;
  - H_3: Rossby waves' amplitudes on the Atlantic are smaller than the ones in other ocean basins on the Southern Hemisphere due to differences in stratification.

Objectives

- **Chapter 2**:
  - Numerically reconstruct the streamfunction using SQG theory and a realistic stratification profile and assess which theory dominates sea surface height over a 14-year time series;
- **Chapter 3**:
  - Identify Rossby waves and assess differences in waves' amplitudes at several spectral bands in the three ocean basins of the Southern Hemisphere;
  - Apply the QG modal decomposition to reconstruct the SSHA and identify differences in Rossby waves' amplitudes.

Chapter 2

What does the altimeter see?

- TOPEX/Poseidon ⟶ first major oceanographic research satellite;

- Most ocean regions were dominated by the barotropic plus the first baroclinic modes, meaning the altimeter reflects the movements of the thermocline [Wunsch, 1997];

- SSH wavenumber spectral slopes in high eddy kinetic energy regions are significantly different from what QG theory predicts [LeTraon et al., 2008];

- Still an ongoing discussion [e.g. Vergara et al., 2019];

Eddy Kinetic Energy (EKE) and wavenumber spectra: a review

- High EKE $\longrightarrow$ SQG theory predictions [e.g. LeTraon et al., 2008];

- Low EKE and between 20°N and 20°S $\longrightarrow$ neither SQG nor QG [e.g. Dufau et al., 2016];

- Increasing latitude, SQG becomes important [e.g. Richman et al., 2012, Vergara et al., 2019].

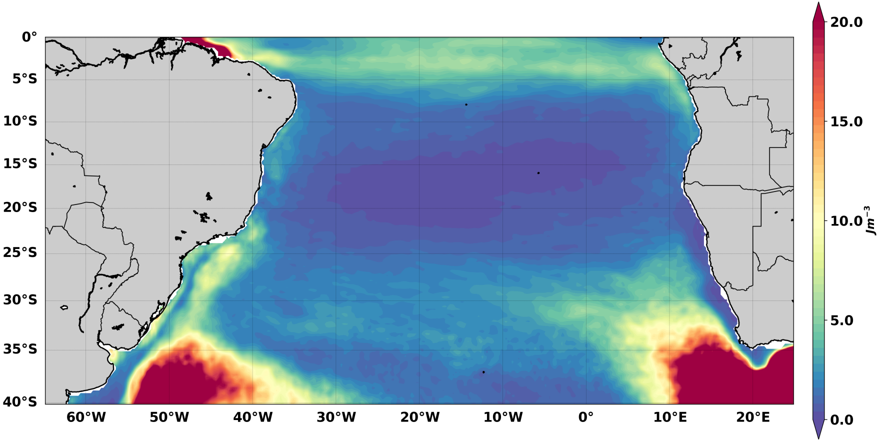

Spatial variance of the geostrophic velocity anomalies in the South Atlantic as a proxy of the EKE (Jm^{-3}).

Study areas

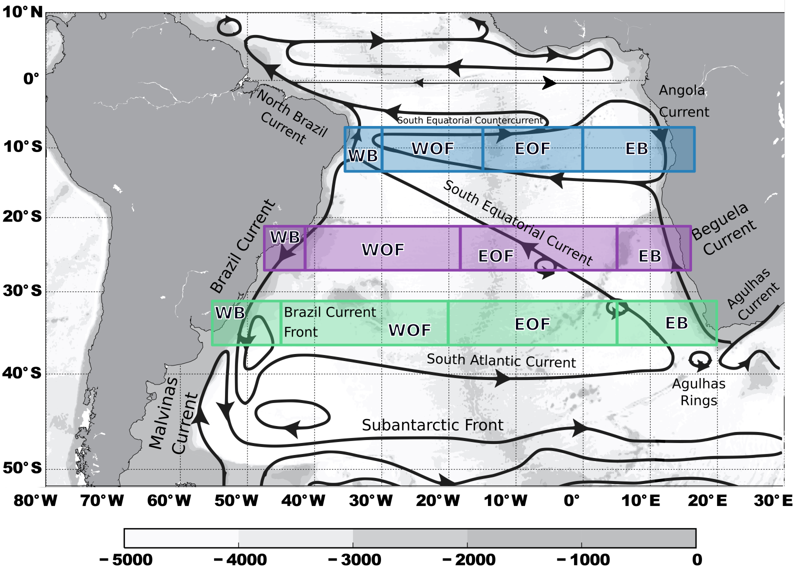

South Atlantic large-scale upper-level geostrophic circulation, adapted from Talley et al. [2011].

SQG solutions: Methods

H_1: The dominance of QG or SQG at 11°S, 24.5°S and 34.5°S in the reconstruction Atlantic's SSH is related to the amount of mesoscale activity in each area;

- HYCOM $\longrightarrow$ assimilates satellites, has better spatial resolution, and T and S profiles are physically consistent with SSH;
- TEOS-10 $\longrightarrow$ T and S converted to conservative temperature and absolute salinity $\longrightarrow$ realistic N^2 and b_s;
- T, S and SSH weekly averaged $\longrightarrow$ mesoscale.

1. Numerically calculated χ ("exact" solution):

$$\frac{\partial}{\partial z}\left(\frac{f_0^2}{N^2}\frac{\partial \chi}{\partial z}\right) - K^2\chi = 0\,;$$

2. Reconstruct ψ_{sqg} in the Fourier domain:

$$\hat{\psi}_{sqg}(\mathbf{k}, z) = \chi(k, z)\,\hat{b}_s(\mathbf{k})\,;$$

3. Filter to retain wavelengths between 12 and 400 km;

4. Assess SQG or QG dominance provided $\psi = \psi_{sqg} + \psi_{int}$:

$$\gamma = \sqrt{\frac{\sum(\psi_{sqg}^2)}{\sum(\psi - \psi_{sqg})^2}}.$$

14 years of SSH reconstruction

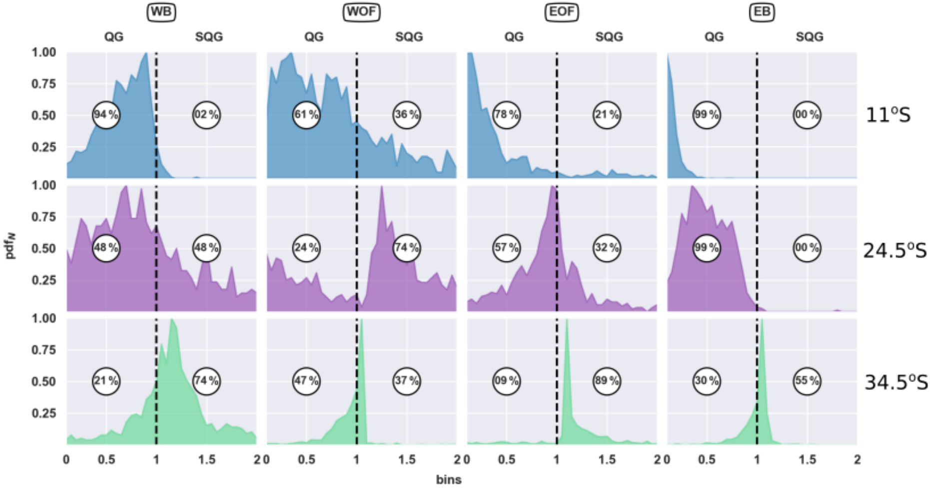
WB
WOF
EOF
EB
QG
SQG
1.00
0.75
0.50
0.25
pdf$_N$
94 %
02 %
61 %
36 %
78 %
21 %
99 %
00 %
11°S
48 %
48 %
24 %
74 %
57 %
32 %
99 %
00 %
24.5°S
21 %
74 %
47 %
37 %
09 %
89 %
30 %
55 %
34.5°S
0
0.5
1
1.5
2
bins

- Deepening of the mixed layer (ML) facilitates ML instabilities [Rocha et al., 2016] $\longrightarrow$ submesoscale fronts energize larger scales;

- Seasonal variations of the ML affect SQG reconstruction [Gonzalez-Haro and Isern-Fontanet, 2014, Sasaki et al., 2014];

- Winter: a deep ML leads to stronger lateral buoyancy gradients [Callies et al., 2015].

- Regime change [Vergara et al., 2019].

	WB		WOF		EOF		EB		
	QG	SQG	QG	SQG	QG	SQG	QG	SQG	Latitude
Summer	91%	2%	72%	27%	100%	0%	100%	0%	11°S
Winter	92%	4%	49%	46%	69%	29%	100%	0%	
Summer	51%	47%	45%	54%	82%	12%	100%	0%	24.5°S
Winter	59%	37%	8%	91%	33%	51%	99%	1%	
Summer	14%	84%	91%	2%	19%	80%	60%	23%	34.5°S
Winter	7%	90%	4%	85%	0%	99%	27%	92%	

Highlights

- QG dominated over most of our study areas;
- SQG dominates in regions where higher EKE is found on the South Atlantic;
- Our SSH reconstruction related to the seasonal variation of the ML, in accordance to Gonzalez-Haro and Isern-Fontanet [2014];
- Seasonal change between the QG $\leftrightarrow$ SQG regimes, corroborating Vergara et al. [2019];
- Increase in SQG dominance poleward, corroborating Richman et al. [2012];

Chapter 3

Quasi-geostrophic interior modes and Rossby waves

Long, internal Rossby waves

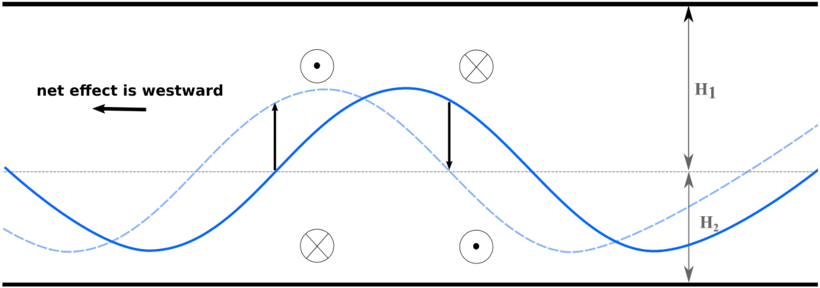

Schematics of a long internal Rossby wave, adapted from Salmon (1998).

- These waves have a clear signal at the surface when displacing the main thermocline [Polito and Cornillon, 1997];
- Found in the three ocean basins, and although presenting similar characteristics at the same latitudes, surface amplitudes are different [Polito and Liu, 2003].

Rossby waves on the Southern Hemisphere

H_2: Most of the variability of the SSHA associated to propagating signals at 11°S, 24.5°S e 34.5°S is explained by Rossby waves;

- Identify Rossby waves in altimeter's SSHA at 11°S, 24.5°S and 34.5°S using Finite Impulsive Response (FIR) filters.

FIR2D filters [Polito et al., 2000, Polito and Liu, 2003]

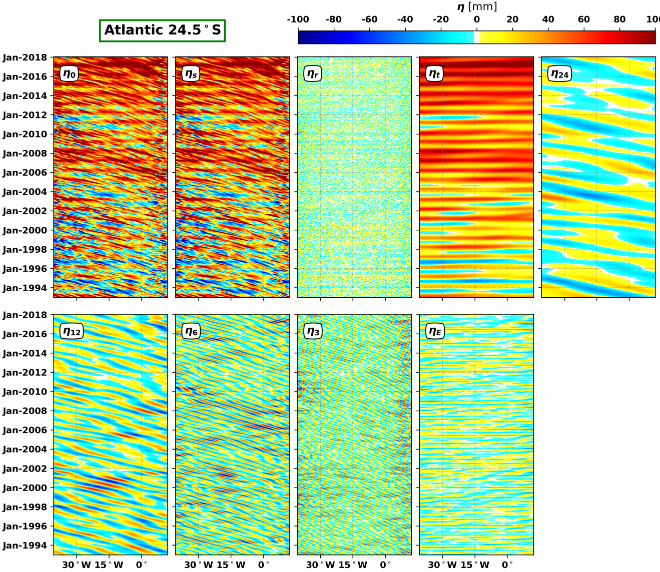

FIR2D filters [Polito et al., 2000, Polito and Liu, 2003]

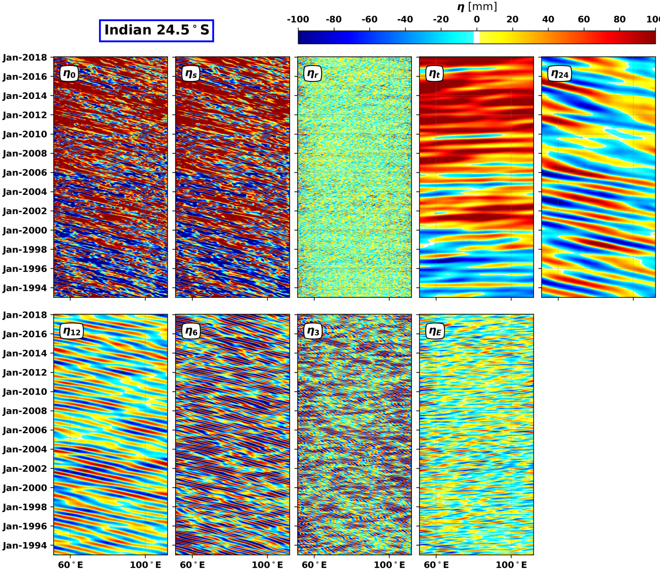

Rossby waves account for **more than half** of the surface signal in most of the cases, being as important as the seasonal cycle!

Basin	Latitude	Rossby waves	η_t
Atlantic	11°S	41%	56%
	24.5°S	**57%**	42%
	34.5°S	**61%**	32%
Pacific	11°S	**63%**	46%
	24.5°S	**73%**	22%
	34.5°S	**51%**	45%
Indian	11°S	**69%**	30%
	24.5°S	**75%**	19%
	34.5°S	**67%**	14%

Explained variance of the sum of all filtered Rossby waves and the seasonal and large scale signal (η_t) for each latitude and basin of the Southern Hemisphere.

QG modes: Methods

H_3: Rossby waves' surface amplitudes on the South Atlantic Ocean are smaller than the ones in other ocean basins due to differences in stratification, although the atmospheric forcing is similar;

- Apply the QG modal decomposition to obtain R_{di} and the vertical structure $F(z)$ for each mode;
- Present the Atlantic, Pacific and Indian Ocean's stratification and vertical structure $F(z)$;
- Reconstruct the SSHA using different, realistic stratification profiles to detect changes in waves' surface amplitudes.

1. T and S from ISAS climatology $\longrightarrow$ N^2, longitudinally averaged;
2. Calculate F_i and R_{di} for the first 3 modes $i = [0, 1, 2]$:

$$\frac{\partial}{\partial z}\left(\frac{f_0^2}{N^2}\frac{\partial F_i}{\partial z}\right) + \lambda_i F_i = 0\,;$$

3. Calculate the modal amplitudes from HYCOM's vertical velocity profiles (u, v) for the first 3 modes $\longrightarrow \Psi_i$;
4. Reconstruct the SSHA,

$$\eta = \frac{f_0}{g}\,\psi = \frac{f_0}{g}\sum_{i=0}^{2}\Psi_i\,F_i\,.$$

Rossby radii of deformation (R_{di}) and dispersion diagram

R_{di} and dispersion relation

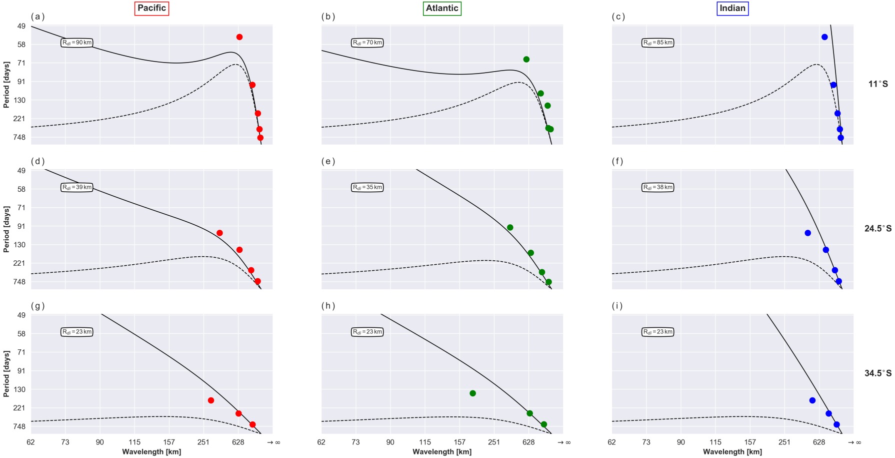

Vertical modes and stratification

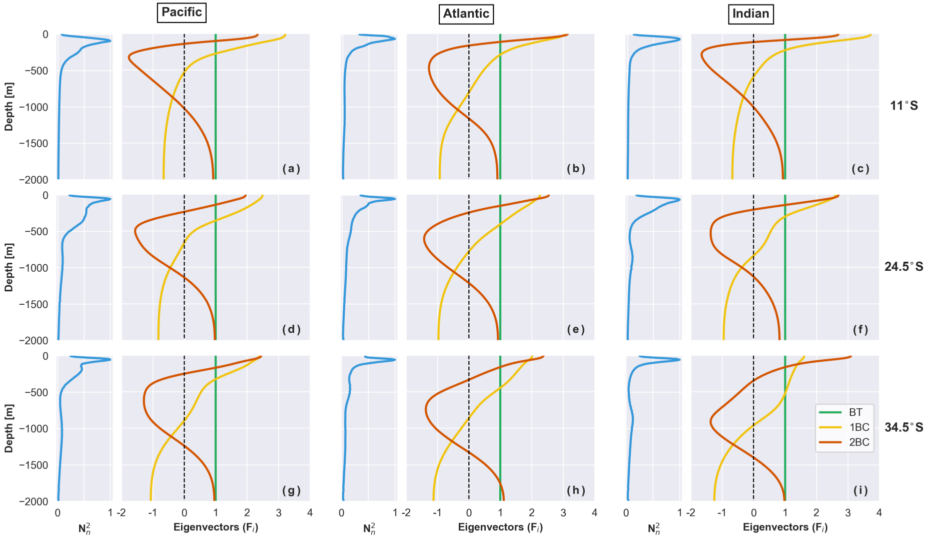
Pacific
Atlantic
Indian
11°S
24.5°S
34.5°S
Depth [m]
(a)
(b)
(c)
(d)
(e)
(f)
(g)
(h)
(i)
BT
1BC
2BC
N_n^2
Eigenvectors (F_i)

SSHA reconstruction

- Determining the modal amplitudes Ψ_i in the Fourier domain from HYCOM's velocities [Silveira et al., 2000];

- For a three mode truncation:

$$\eta = \frac{f_0}{g}\,\psi = \frac{f_0}{g}\sum_{i=0}^{2} \Psi_i\, F_i\,.$$

Explained variance for each modal component to the total ψ.

Basin	Latitude	BT	**BC1**	BC2	BT + BC1 + BC2
Atlantic	11°S	35%	**70%**	15%	84%
	24.5°S	57%	**67%**	3%	87%
	34.5°S	75%	**79%**	9%	91%
Pacific	11°S	40%	**75%**	2%	83%
	24.5°S	64%	**86%**	6%	92%
	34.5°S	75%	**83%**	19%	88%
Indian	11°S	55%	**89%**	9%	94%
	24.5°S	74%	**90%**	12%	96%
	34.5°S	81%	77%	5%	93%

Explained variance for each modal component to the total ψ.

Basin	Latitude	BT	**BC1**	BC2	BT + BC1 + BC2
Atlantic	11°S	35%	**70%**	15%	84%
	24.5°S	57%	**67%**	3%	87%
	34.5°S	75%	**79%**	9%	91%
Pacific	11°S	40%	**75%**	2%	83%
	24.5°S	64%	**86%**	6%	92%
	34.5°S	75%	**83%**	19%	88%
Indian	11°S	55%	**89%**	9%	94%
	24.5°S	74%	**90%**	12%	96%
	34.5°S	81%	77%	5%	93%

Sea surface height anomaly reconstruction

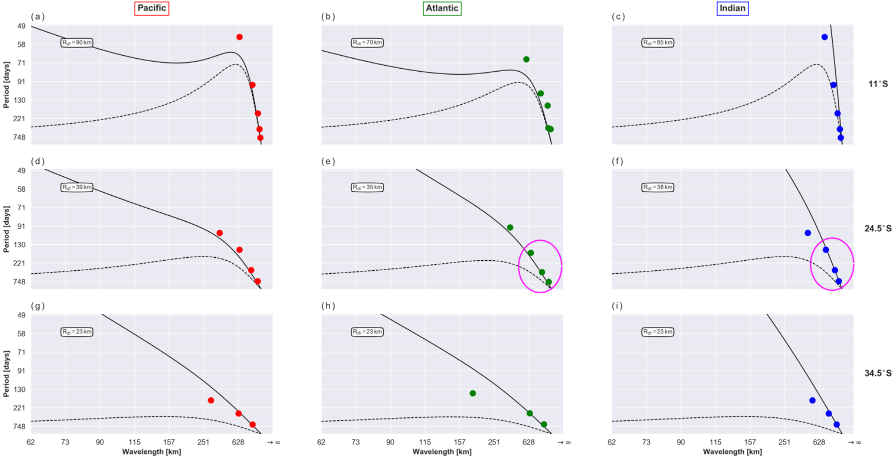

An example at 24.5°S

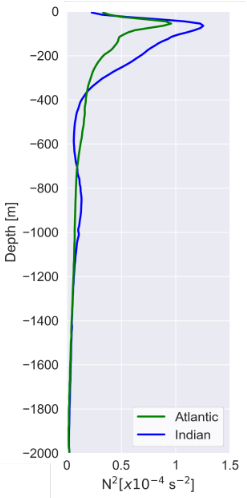

- Approximately the center of subtropical gyres in all basins;
- Mean currents and shear are smaller compared to other locations;
- It is a region between the trade winds and the westerlies, so the wind contribution is relatively weak;
- For these linear waves, the only difference between basins is N^2.

Sea surface height anomaly reconstruction

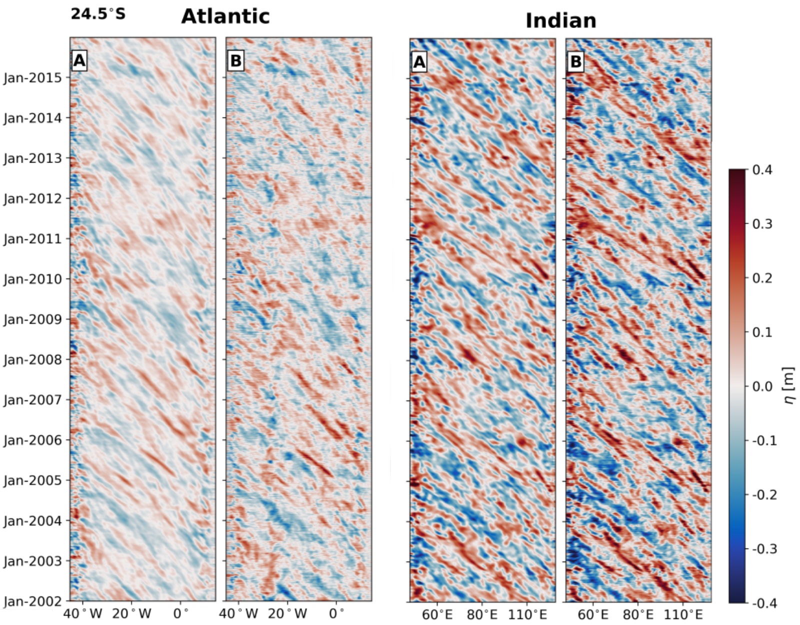

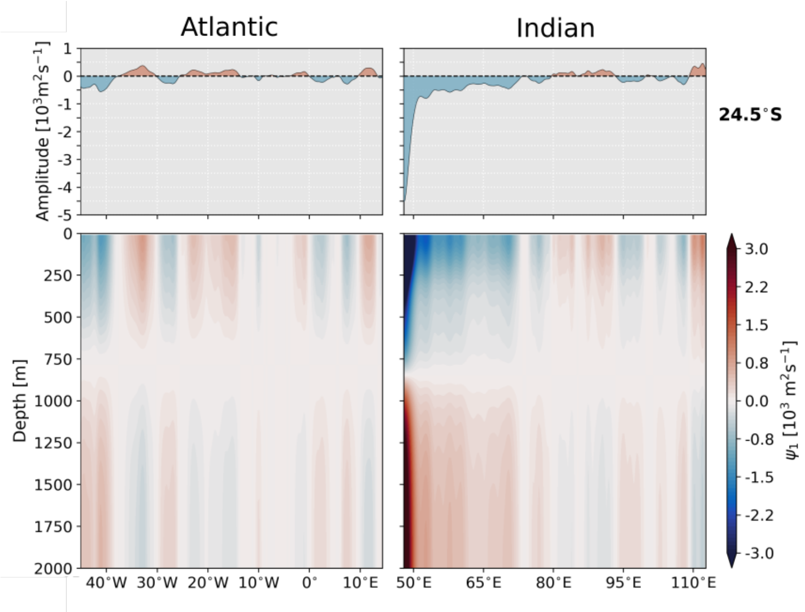
Atlantic
Indian
24.5°S
Amplitude [$10^3 m^2 s^{-1}$]
1
0
-1
-2
-3
-4
-5
Depth [m]
0
250
500
750
1000
1250
1500
1750
2000
40°W 30°W 20°W 10°W 0° 10°E
50°E 65°E 80°E 95°E 110°E
3.0
2.2
1.5
0.8
0.0
-0.8
-1.5
-2.2
-3.0
ψ_1 [10^3 $m^2 s^{-1}$]

What if we replace the Atlantic stratification with the Indian one?

- Reconstruct the Atlantic's SSHA using the Indian vertical structures;
- FIR2D $\longrightarrow$ compare new amplitudes to the ones obtained from the unchanged Atlantic.

Result: surface amplitudes doubled!

Highlights

- Rossby waves explain most of the SSHA signal at 11°S, 24.5°S, and 34.5°S, being as important as the seasonal cycle;
- Most of the Rossby waves captured by the altimeter are linear, of the first baroclinic mode and Doppler shifted;
- A three mode truncation suffices to reproduce most of the SSHA signal in all basins and latitudes;
- **Stratification can modulate Rossby waves' surface amplitudes**.

Final remarks

Final Remarks

- SQG dominates where EKE is higher and with increasing latitude on the South Atlantic $\longrightarrow$ we **confirm** hypothesis H_1;
- Westward propagating features explained from 41% to 75% of the total sea level anomaly field in all latitudes and basins $\longrightarrow$ we **confirm** hypothesis H_2;
- In most cases a more (less) stratified water column lead to larger (smaller) surface amplitudes; where waves are non-linear and where stratification profiles are similar, differences in amplitudes were smaller among basins $\longrightarrow$ we **confirm** hypothesis H_3.

Final Remarks

- SQG dominates where EKE is higher and with increasing latitude on the South Atlantic $\longrightarrow$ we **confirm** hypothesis H_1;
- Westward propagating features explained from 41% to 75% of the total sea level anomaly field in all latitudes and basins $\longrightarrow$ we **confirm** hypothesis H_2;
- In most cases a more (less) stratified water column lead to larger (smaller) surface amplitudes; where waves are non-linear and where stratification profiles are similar, differences in amplitudes were smaller among basins $\longrightarrow$ we **confirm** hypothesis H_3.

Final Remarks

- SQG dominates where EKE is higher and with increasing latitude on the South Atlantic $\longrightarrow$ we **confirm** hypothesis H_1;
- Westward propagating features explained from 41% to 75% of the total sea level anomaly field in all latitudes and basins $\longrightarrow$ we **confirm** hypothesis H_2;
- In most cases a more (less) stratified water column lead to larger (smaller) surface amplitudes; where waves are non-linear and where stratification profiles are similar, differences in amplitudes were smaller among basins $\longrightarrow$ we **confirm** hypothesis H_3.

Thank you!

Instituto Oceanográfico

CNPq
Conselho Nacional de Desenvolvimento
Científico e Tecnológico

FAPESP

LOS
Laboratório de
Oceanografia por
Satélites

Institut
de Ciències
del Mar

References

J. Callies, R. Ferrari, J. M. Klymak, and J. Gula. Seasonality in submesoscale turbulence. *Nature communications*, 6(1):1–8, 2015.

C. Dufau, M. Orsztynowicz, G. Dibarboure, R. Morrow, and P.-Y. LeTraon. Mesoscale resolution capability of altimetry: Present and future. *Journal of Geophysical Research: Oceans*, 121:4910–4927, 2016.

C. Gonzalez-Haro and J. Isern-Fontanet. Global ocean current reconstruction from altimetric and microwave sst measurements. *Journal of Geophysical Research: Oceans*, 119:3378–3391, 2014.

P. Y. LeTraon, P. Klein, B. L. Hua, and G. Dibarboure. Do altimeter wavenumber spectra agree with the interior or surface quasigeostrophic theory? *Journal of Physical Oceanography*, 38:1137–1142, 2008.

P. S. Polito and P. Cornillon. Long baroclinic Rossby waves detected by topex/poseidon. *Journal of Geophysical Research*, 102:3215–3235, 1997.

P. S. Polito and W. Timothy Liu. Global characterization of Rossby waves at several spectral bands. *Journal of Geophysical Research*, 108 (C1):1–18, 2003.

P. S. Polito, O. T. Sato, and W. Timothy Liu. Characterization and validation of the heat storage variability from TOPEX/Poseidon at four oceanographic sites. *Journal of Geophysical Research*, 105(C7):16911–16921, 2000.

J. G. Richman, B. K. Arbic, J. F. Shriver, E. J. Metzger, and Alan J. Wallcraft. Inferring dynamics from the wavenumber spectra of an eddying global ocean model with embedded tides. *Journal of Geophysical Research*, 117(C12012):1–11, 2012.

C. B. Rocha, S. T. Gille, T. K. Chereskin, and D. Menemenlis. Mesoscale to submesoscale wavenumber spectra in Drake Passage. *Journal of Physical Oceanography*, 46:601–620, 2016.

H. Sasaki, P. Klein, B. Qiu, and Y. Sasai. Impact of oceanic-scale interactions on the seasonal modulation of ocean dynamics by the atmosphere. *Nature: Communications*, 5(5636):1–8, 2014.

I. C. A. Silveira, W. S. Brown, and G. R. Flierl. Dynamics of the North Brazil Current retroflection region from the western Tropical Atlantic Experiment observations. *Journal of Geophysical Research*, 105(C12):28559–28583, 2000.

L. D. Talley, G. L. Pickard, W. J. Emery, and J. H. Swift. *Descriptive Physical Oceanography: An Introduction*. Elsevier, sixth edition edition, 2011.

O. Vergara, R. Morrow, I. Pujol, G. Dibarboure, and C. Ubelmann. Revised global wave number spectra from recent altimeter observations. *Journal of Geophysical Research: Oceans*, 124:3523–3537, 2019.

C. Wunsch. The vertical partition of oceanic horizontal kinetic energy. *Journal of Physical Oceanography*, 27:1770–1794, 1997.